Design of a Ventilation System Coupled with a Horizontal Air-Ground Heat Exchanger (HAGHE) for a Residential Building in a Warm Climate

Authors:

Cristina Baglivo, Delia D'Agostino, Paolo Maria Congedo

Abstract:

Energy consumption in new buildings can be reduced at the design stage. This study optimizes the ventilation system design of a new residential building located in a warm climate (Southern Italy). Different system options of horizontal air-ground heat exchangers (HAGHEs), also called earth-to-air heat exchangers (EAHX), have been considered to search for the optimal configuration. The thermal behaviour of the obtained configurations has been modelled by the dynamic simulation software TRNSYS 17. The pipe numbers, the air flow rate, and the soil thermal conductivity are among the simulated building components. For each of them, different design options have been analysed to study how each parameter impacts the building thermal behaviour in winter and summer. The operative air temperature (TOP) has been evaluated inside the building prototype to investigate the indoor comfort. The paper demonstrates that HAGHEs permit to assure a suitable indoor climatization if the building envelope is optimized for a warm area. These conditions require high values of heat storage capacity to keep under control the internal temperature fluctuations, especially in summer. The paper confirms the importance of geothermal systems and design optimization to increase energy savings.

Design of a Ventilation System Coupled with a Horizontal Air-Ground Heat Exchanger (HAGHE) for a Residential Building in a Warm Climate

Cristina Baglivo [1], Delia D'Agostino [2,*] [ID] and Paolo Maria Congedo [1] [ID]

[1] Department of Engineering for Innovation, University of Salento, 73100 Lecce, Italy;
cristina.baglivo@unisalento.it (C.B.); paolo.congedo@unisalento.it (P.M.C.)

[2] European Commission, Joint Research Centre (JRC), Directorate-C-Energy, Transport and Climate, Energy Efficiency and Renewables Unit, Via E. Fermi 2479, 21027 Ispra, Italy

* Correspondence: delia.dagostino@ec.europa.eu

check for updates

Abstract: Energy consumption in new buildings can be reduced at the design stage. This study optimizes the ventilation system design of a new residential building located in a warm climate (Southern Italy). Different system options of horizontal air-ground heat exchangers (HAGHEs), also called earth-to-air heat exchangers (EAHX), have been considered to search for the optimal configuration. The thermal behaviour of the obtained configurations has been modelled by the dynamic simulation software TRNSYS 17. The pipe numbers, the air flow rate, and the soil thermal conductivity are among the simulated building components. For each of them, different design options have been analysed to study how each parameter impacts the building thermal behaviour in winter and summer. The operative air temperature (TOP) has been evaluated inside the building prototype to investigate the indoor comfort. The paper demonstrates that HAGHEs permit to assure a suitable indoor climatization if the building envelope is optimized for a warm area. These conditions require high values of heat storage capacity to keep under control the internal temperature fluctuations, especially in summer. The paper confirms the importance of geothermal systems and design optimization to increase energy savings.

Keywords: geothermal; zero energy buildings (ZEBs); thermal comfort; earth-to-air heat exchanger (EAHX)

Highlights

- The ventilation system of a residential building is investigated in a warm climate.
- The design of a Horizontal Air-Ground Heat Exchanger is optimized.
- Different HAGHE configurations have been modelled and compared.
- The operative air temperature (TOP) has been evaluated inside the building.
- The optimized HAGHE system assures a proper indoor ventilation.

1. Introduction

Containing greenhouse gas emissions and climate change is a global priority [1]. At the European level, the improvement of energy efficiency in buildings has become the focus of energy and climate policies [2,3]. The recast of the Energy Performance of Buildings (EPBD) Directive (EU, 2010/31/EU), the Energy Efficiency Directive (EED) (EU, 2012/27/EU), and the Renewable Energy Directive (RED) (EU, 2009/28/EU) constitute the European framework to reduce energy consumption in buildings [4–6].

Energy consumption can be significantly reduced if the suitability of potential technical solutions is established in a comprehensive manner at the design stage [7–9]. A simulation-based optimization

approach is a promising tool developed to find an appropriate building design [10]. These tools that can cover a wide range of applications with the purpose of reducing energy consumption investigating different design variables [11,12]. Some applications deal with HVAC, ventilation, and photovoltaic (PV) systems [13,14]. Studies have been developed to optimize a single building component, such as windows or envelope [15,16], comfort, and relative humidity [17,18]. A simulation-based optimization approach has the advantage of evaluating specific design options dealing with many measures and maintaining a manageable calculation scheme [19,20].

Valdiserri et al. [21] show the analysis of the ventilation system in a building focusing on the quality of the indoor air, considering that it is an important aspect to guarantee a healthy internal environment. The study of Lucchi et al. [22] focuses on the ground source heat pump (GSHP) as the generation system through numerical simulations, highlighting that GSHP systems adequately meet the requests of the European directive on the issues of use of renewable energy technologies for space heating and cooling.

This study optimizes the ventilation system of a new residential building located in a warm climate. A horizontal air-ground heat exchanger (HAGHE) has been tested in terms of indoor operative air temperature (TOP) and thermal comfort. The number of the pipes, the air flow rate, the thermal conductivity of the soil and the length of the pipes are among the investigated building components. The research aim is to reduce energy consumption and air-conditioning with only the use of the HAGHEs, which exploit the energy stored underground to pre-heat or pre-cool the air that goes in the building, depending on climate.

1.1. Building Optimal Design in a Warm Climate

The energy performance in buildings is the result of the synergy of several elements including location, climate, costs, available resources and materials [23]. Being responsible for more than 70% of the total heat losses, the envelope design results essential to reach a high energy performance. Depending on climate, the envelope air-tightness can be improved to minimise air leakage. However, a minimum air exchange in the building is required to maintain indoor air quality and comfort, although tight construction with enthalpy recovery can produce large savings [24].

In cold climates, multi-layered walls with a low steady thermal transmittance are chosen with low density and high thickness insulating materials. This allows to reduce heating over cold winters, when the preservation of the indoor heat is crucial [25]. Several studies have dealt with the technical, environmental and economic effectiveness of energy efficiency measures in a warm climate [26–29]. In highly efficient buildings, the most suitable technologies are used with optimum design techniques to minimize summer heat gains and winter heat losses. Thermal insulation can guarantee reduced thermal losses and at the same time renewable energy production can balance energy consumption. Low-solar gain windows are generally preferred in warm climates while high-solar gain windows are favoured in cold climates [28].

Different studies [30–33] point out the characteristics of sustainable materials, defining them consist of a high recycled and reused content, rapidly renewable periods and low-emitting contaminants. Indeed, these materials are preferable because they are low consuming and reparable, safe to use, easy to build with, and highly satisfying to the final user. Some applications focus on high efficiency walls favouring the use of local, natural materials and prefabricated systems [34,35].

In a previous study [36], the authors of this paper investigated the envelope of a building located in a warm climate. Results show how an extensive insulation thickness is not necessary in this climate while a high value of the internal aerial heat capacity is important to guarantee a high massive envelope. Low values of the decrement factor and high values of the time shift are preferred in this climate. Especially in summer, external walls with high values of internal aerial capacity can reduce and delay temperature peaks towards the internal side of the building. Different design components can be considered within the optimization to reduce energy consumption. A high risk of internal overheating

characterizes this climate. For this reason, monitoring solar radiation and managing free gains are both important to guarantee a high level of comfort.

1.2. Horizontal Air-Ground Heat Exchangers (HAGHEs)

Geothermal systems are technological measures able to enhance the energy performance of buildings reducing energy consumption. Horizontal air-ground heat exchangers (HAGHEs) are composed of an underground pipe located close to a building and connected to it. The system exploits a simple physics property: ground temperature is almost constant throughout the year, being lower than the outdoor temperature in summer and higher in winter. This temperature difference can be used to pre-cool (in summer) or pre-heat (in winter) the air passing through the system before entering a building. The air leaving the pipe can be used for ventilation and for handling thermal loads, partially, or totally. The soil physical properties and the climatic conditions of a site influence the system performance [37] that has been investigated in different Italian climates [38]. Good results have been obtained in cold climates where re-heating the HAGHE air downstream was found necessary before supplying air in a building, while indoor comfort conditions were achieved without re-cooling in summer [39]. In this season, it was possible to implement free-cooling avoiding the post-treatment with heat pumps [40]. A ground source heat pump (GSHP) contributes to the CO_2 reduction resulting in a good investment, especially for large buildings [41]. This system also decreases primary energy consumption up to 60% compared to other systems [42–44]. Furthermore, Desideri et al. [45] have shown how the GSHP leads to lower operating costs.

HAGHEs can be autonomous or hybrid when used in combination with a conventional heating or cooling system [46,47]. The exchange of air with the ground can take place through vertical or horizontal exchangers [48]. The first option is preferred when the external area of the building is limited. A deeper burial depth of the pipes implies a minor influence of the atmospheric agents. The pipes should be spaced at least 1.5 m with a burial depth between 1.2 m and 1.8 m in horizontal systems to avoid a thermal exchange between them [49].

The analysis developed in [50] shows the real advantages in the use of HAGHEs in buildings located in warm areas during the summer season, also with short pipes. On the contrary, advantages in winter become important only during a few hours in a day. The studies presented in [51–53] investigate how different parameters impact the HAGHEs behaviour through CFD simulations. The analysis investigated several geometrical configuration options and examined various parameters like ground thermal conductivity, heat transfer fluid velocity and depth installation.

In this paper the HAGHE suitability is tested, investigating the internal operative air temperature (TOP) in a building located in a warm climate.

2. Methodology

The methodology of this paper is aimed at the optimization of the system design of a new residential building located in a warm climate. A horizontal air-ground heat exchangers (HAGHEs) has been considered as the ventilation system. The building has been modelled to evaluate the internal operative air temperature (TOP). Different building configurations have been obtained with a variable HAGHE pipe number, air flow rate, soil thermal conductivity, and pipe depth. Once the best performing option of one component is identified, this is incorporated in following simulations of the model. In this way, the most efficient system is sequentially designed in relation to the simulated options. The thermal building behaviour of each system design option has been studied in both winter and summer. The TOP trends have been analysed to determine how the geothermal system options impact the internal comfort.

2.1. The Building Modeling

The building has been modelled using the dynamic simulation software TRNSYS 17 (Transient System Simulation) (University of Wisconsin–Madison, Madison, WI, USA) [54]. The building

components have assembled using the graphical interface TRNSYS Simulation Studio. The model inputs and outputs have been introduced through the TRN Build interface. The software code allows to calculate the thermal behaviour of the building components that are defined by types. This study has been carried out by the following types, linked for the model set up, as shown in Figure 1:

- Building information on envelope, walls, stratigraphy, materials, floor, roof, windows, and thermal loads (Type 56);
- Soil characteristics (Type 77);
- Weather data (Type 15) including the weather data of the location (data generated by Meteonorm);
- Single Pipe System in GHP (Geothermal Heat Pump) Library (Type 952);
- Time forcing function, varying from 0 (system turned off) to 1 (system turned on) (Type 14h).
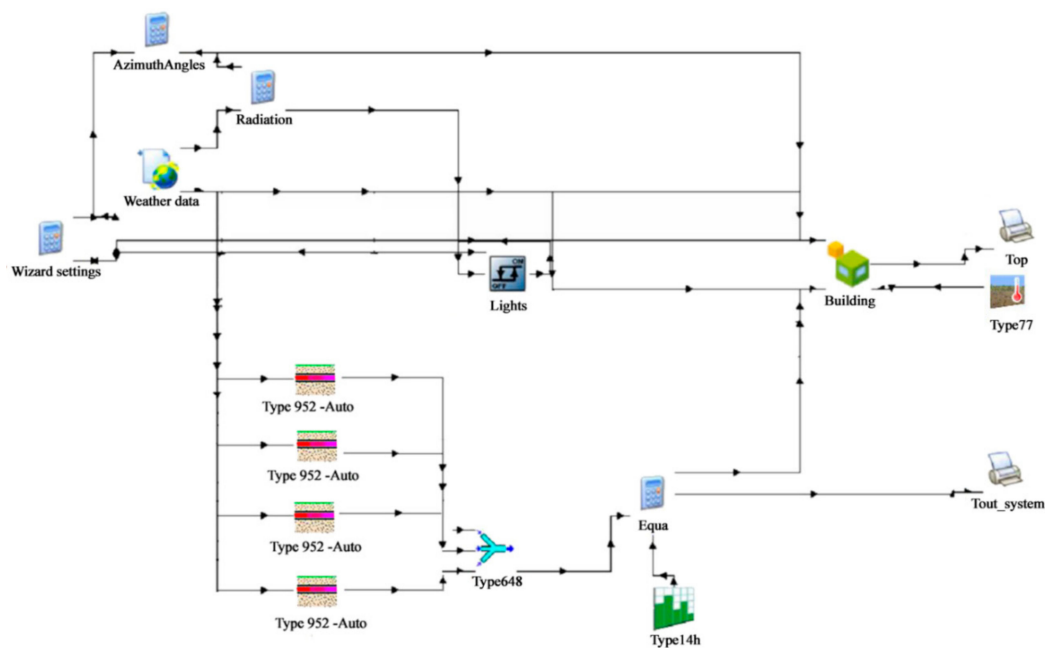
Figure 1. TRNSYS 17 simulation scheme for building energy analysis.

Type 952 models a pipe buried under the ground surface. The buried pipe is surrounded by a three-dimensional finite difference conduction network in order to calculate the heat build-up in the ground. The setup parameters of Type 952 are shown in Table 1, in particular:

- "Mean surface temperature" is the mean temperature of the air at zero altitude;
- "Amplitude of surface temperature" indicates the difference between the maximum temperature and the mean temperature (related to the temperature of the air at zero altitude);
- "Time shift" is the difference between the first day of the year and the day when there is the lowest annual temperature in a specific location.

The "Number of Radial Soil Nodes" is equal to −1 because the software sets this value to a negative number when the model will calculate the radial noding pattern based on an expanding multiplier. At the end of Table 1, the parameters for setting the finite elements calculations have been shown.

Table 1. Configuration parameters of HAGHE.

Pipe Parameters	Nominal Diameter	0.2	m
	Thermal Conductivity of Pipe Material	0.40	W/mK
Air Parameters	Density of Air	1.205	kg/m^3
	Thermal Conductivity of Air	0.026	W/mK
	Specific Heat of Air	1.005	kJ/kgK
	Viscosity of Air	1.81×10^{-5}	kg/ms
	Initial Temperature of Air	10.1	°C
Ground Parameters	Ground Thermal Conductivity	1	W/mK
		2	W/mK
		3	W/mK
	Density of Ground	2723	kg/m^3
	Specific Heat of Ground	0.837	kJ/kgK
	Average Surface Temperature	16.7	°C
	Amplitude of Surface Temperature	18.8	°C
	Time Shift	45	day
Finite Elements Calculation Set up	Number of Fluid Nodes	200 (L = 20 m)	-
		250 (L = 25 m)	-
		300 (L = 30 m)	-
		400 (L = 40 m)	-
		500 (L = 50 m)	-
	Number of Radial Ground Nodes	−1	-
	Number of Axial Ground Nodes	20	-
	Number of Circumferential Ground Nodes	8	-
	Smallest Node Size	0.2	m
	Node Size Multiplier	1.2	-
	Farfield Distance	1	m

2.2. The Case Study

The case study is a residential building prototype placed in a warm area characterized by non-extreme winters and high aridity summers. This climate is common in some Italian regions, such as Puglia, Sicily and Calabria. The building is in Brindisi, a Southern Italian city belonging to the national climatic zone C, having 1083 heating degrees day (HDD) and 299 cooling degree day (CDD). In this zone, the required indoor temperature is set at 20 °C during the heating period (from 15 November to 31 March) and 26 °C during the cooling period (from 25 June to 30 August).

The building has a square plan having a net surface of 225 m^2 and net height of 2.7 m. As shown in Figure 2, it has been divided into nine equal-sized modules of 5 m × 5 m. Each module is a thermal zone with a specific orientation. This division allows the evaluation of the operative air temperature and the thermal behaviour inside the building. The nine thermal zones are divided from each other by internal tuff walls of 12 cm thick.

The building envelope has been optimized, and described in details, in a previous research work [28]. It has been designed to keep under control the internal gains, especially during the summer months.
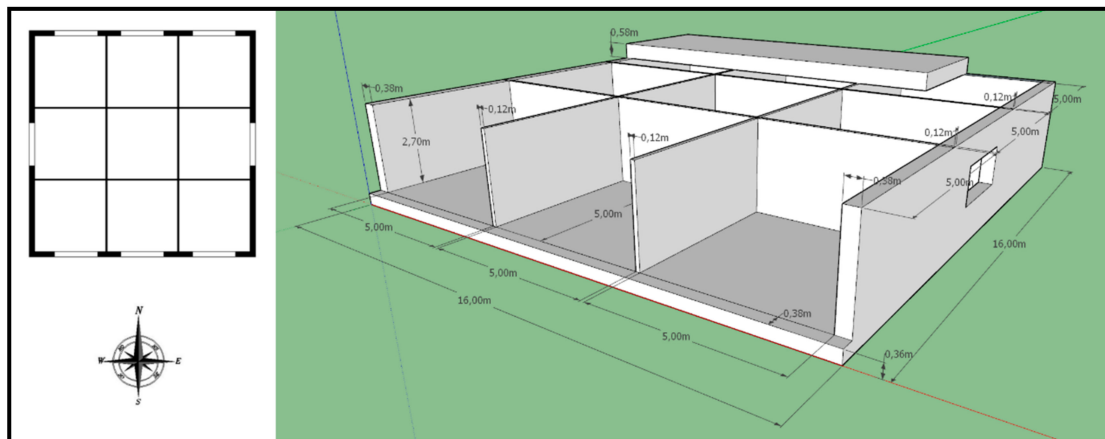
Figure 2. Case study representation.

In Figure 3, an example of the layout of the horizontal air-ground heat exchanger has been shown. For each combination, number and length of pipes can be changed, while the depth of the installation is always the same.
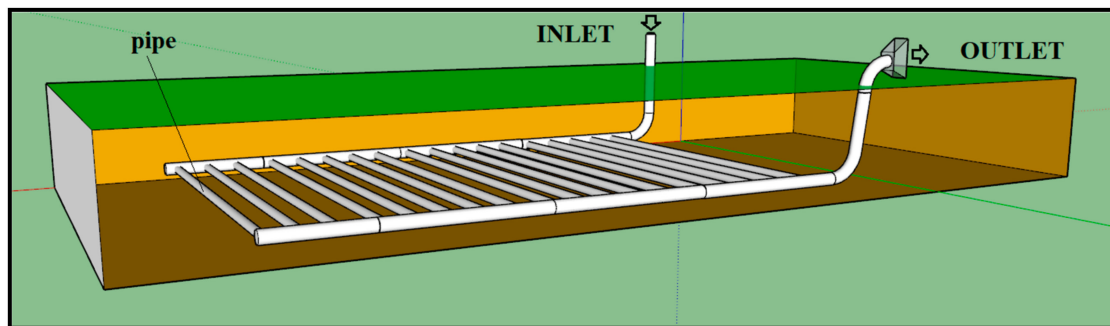
Figure 3. The layout of the horizontal air-ground heat exchangers.

Table 2 shows the thermal properties and thicknesses of each building material. These properties are useful for the evaluation of the steady and dynamic behaviour of the components.

Table 2. Thermo-physical properties of building materials.

Properties	Material	(W/m·K)	c (J/Kg·K)	ρ (kg/m^3)	Thickness (cm)
Wall (Internal to External Side)	Tuff	1.7	850	2300	10
	Brick	0.13	1000	600	20
	Polystyrene	0.034	1700	35	8
Ground Floor	Stoneware flooring	1.47	850	1700	1.5
	Concrete (1200 kg/m^3)	0.47	850	1200	8
	Concrete (1600 kg/m^3)	0.73	850	1600	5
	Igloo	0.072	850	1000	16
	Screed ordinary concrete	1.06	850	1700	5
	Gravel	1.2	850	1700	1
Ceiling	Hollow-core concrete	0.743	850	1800	25
	Concrete (400 kg/m^3)	0.19	850	400	10
	XPS polystyrene panel	0.04	850	35	8
	Tuff	1.7	850	2300	10
	Bricks tuff	0.55	850	1600	5

The external walls consist of three layers (excluding the plaster layer) able to maintain a capacitive behaviour. As shown in Table 3, the external walls have been chosen with a high internal areal heat capacity (80.43 kJ/m^{2}K), high mass value (352.8 kg/m^2), low decrement factor (0.078), and low dynamic transmittance (0.019 W/m^{2}K).

Table 3. Envelope characteristics.

Properties	Material	U W/m^{2}K	Y$_{12}$ W/m^{2}K	Y$_{22}$ W/m^{2}K	Y$_{11}$ W/m^{2}K	f$_d$	M$_s$ Kg/m^2	Δt h	k$_1$ kJ/m^{2}K	k$_2$ kJ/m^{2}K	dm
Wall (Internal to External Side)	tuff brick polystyrene	0.243	0.019	0.423	5.841	0.078	352.8	14.53	80.43	5.93	0.38
Ground Floor (Internal to External Side)	stoneware flooring concrete (1200 kg/m^3) concrete (1600 kg/m^3) igloo screed ordinary concrete gravel	0.349	0.016	3.62	3.982	0.047	463.5	19.44	3.982	3.62	0.365
Ceiling (Internal to External Side)	hollow-core concrete concrete (400 kg/m^3) xps polystyrene panel tuff bricks tuff	0.314	0.012	7.39	4.50	0.039	803	17.93	61.8	101.6	0.580

The position of the insulating layer in the external wall is crucial for the thermal response of the building. In particular, the insulation placed on the outside walls gives the maximum thermal capacity and permits to keep the internal temperature fluctuations at the minimal level. When the insulating layer is in the middle, the thermal capacity of the wall is half in comparison with the previous case. On the other hand, a low heat capacity and very high internal thermal fluctuations are obtained when the thermal insulation is on the internal side.

As shown in Table 3, the ground floor has been designed without the insulation layer. This allows maintaining a higher heat storage capacity, useful for the warm climate.

Windows can significantly impact the average radiant temperature and the internal comfort conditions in buildings. The transparent elements can contribute to the building energy performance providing a pleasant visual effect at the same time. In addition, large window areas can reduce heat loss. Table 4 shows the window properties of the studied building. A window having 6/16/6 low emission glass with Argon in the cavity (g = 0.333) and an aluminum frame is used.

Table 4. Window properties.

Window Measures	Ug (W/m^{2}K)	g	% Frame	Uf (W/m^{2}K)
6/16/6 argon	1.3	0.333	15	2.27

Table 5 shows the internal gains set in the model in terms of number of occupants, artificial lighting, and electronic equipment.

Table 5. Boundary conditions.

Descriptions	Values	Hour	
		from	to
Number of occupants	4	0:00	24:00
Internal gains of occupants	100 W	0:00	24:00
Artificial lighting	5 W/m^2	8:00	20:00
Electronic equipment	3 W/m^2	0:00	24:00

2.3. The Calculation Method

The calculation method has been divided into sixth steps. Table 6 summarizes the objectives of each step and how combinations have been assembled. The list of combinations and the detail of the implemented measures in each combination are presented in Table 7.

Table 6. Development of the methodology.

First step	Different ground thermal conductivity evaluation (no geothermal system)	Combo 1, 2, 3
Second Step	Analysis of the internal ventilation for different ground thermal conductivities (no geothermal system)	Combo 1v, 2v, 3v
Third Step	Analysis of different single pipe flow rates	Combo 2, 2v, 4, 5, 6
Fourth Step	Evaluation of the number of pipes	Combo 6, 7
Fifth Step	Study of the length of the pipe	Combo 6, 8, 9, 10
Sixth Step	Different ground thermal conductivity evaluation (geothermal system)	Combo 11, 12

Table 7. List of combinations.

Combo	Haghe	Number of the Pipes for Room	Total Number of the Pipes	Single Pipe Flow Rate (m^3/h)	Total Flow Rate (m^3/hr)	Pipe Length (m)	Soil Thermal Conductivity (W/mK)
Combo 1	no	-	-	-	-	-	1
Combo 2	no	-	-	-	-	-	2
Combo 3	no	-	-	-	-	-	3
Combo 1v	no	-	-	-	160	-	1
Combo 2v	no	-	-	-	160	-	2
Combo 3v	no	-	-	-	160	-	3
Combo 4	yes	2	18	150	2700	50	2
Combo 5	yes	2	18	187.5	3375	50	2
Combo 6	yes	2	18	225	4050	50	2
Combo 7	yes	4	36	112.5	4050	25	2
Combo 8	yes	2	18	225	4050	40	2
Combo 9	yes	2	18	225	4050	30	2
Combo 10	yes	2	18	225	4050	20	2
Combo 11	yes	2	18	225	4050	50	1
Combo 12	yes	2	18	225	4050	50	3

The simulations have been performed considering the geothermal system turned on from 8:00 a.m. to 8:00 p.m. (12 h). The building prototype has been modelled for a period of one year. The optimization process allows the understanding of the impact of the ventilation system, coupled with HAGHE, on the thermal behaviour of the building. Combining the different design options, 15 combinations (Combo) have been obtained.

The first step studies the TOP behaviour inside the building without HVAC systems, only by varying the ground thermal conductivity. In particular, no ventilation has been considered, as if building were not inhabited. Different values of the ground thermal conductivity have been investigated (1–3 W/mK) in three different combinations (Combo 1, Combo 2, and Combo 3), respectively. The slab on ground floor of the reference building is considered without insulation. Consequently, the heat exchange takes place directly with the ground in function of thermal ground conductivity. This is an extreme limit case, the building is completely sealed, the aim is the analysis of the only building-ground exchange.

In the second step, the natural ventilation has been considered with a total flow rate equal to 160 m^3/h for the entire building. Combo 1v, Combo 2v, and Combo 3v have the ground thermal conductivity equal to 1–3 W/mK, respectively. Additionally, in this case, the HAGHE system has not

been considered. The aim of this choice is the evaluation of the difference in terms of TOP with the previous step (without ventilation) and the next ones with the HAGHE system.

In the third step, a geothermal system characterized by two pipes of 50 m length and 20 cm internal diameter, buried at 2 m depth, has been added in the tested combinations. This step analyses the variation of the air flow rate through the pipes, considering the following values: 150 m^3/h (Combo 4), 187.5 m^3/h (Combo 5), 225 m^3/h (Combo 6). Combo 2 and Combo 2v, which result from the previous step, are also considered for this comparison. The ground thermal conductivity is set at an intermediate and cautionary value equal to 2 W/m K in all the tested combinations.

The fourth step investigates the influence of the system pipe number and length on the TOP inside the building. The variation of the pipe number has been studied. Two pipes of 50 m length and four pipes of 25 m length, having the same air flow rate inlet, have been considered. In this step, an inlet flow rate of 225 m^3/h and a total geothermal system length of 100 m have been investigated. The comparison has been carried out between Combo 6 (two pipes of 50 m) and Combo 7 (four pipes of 25 m).

The fifth step studies how the variation of the pipe length has an impact on the TOP. A flow rate of 112.5 m^3/h has been set at the inlet. Furthermore, the temperature at the pipe outlet has been considered as varying with the purpose of analysing the temperature variation along the pipe. The following combinations have been studied in this step: four pipes of 50 m (Combo 6); four pipes of 40 m (Combo 8); four pipes of 30 m (Combo 9); and four pipes of 20 m (Combo 10). The aim is the evaluation of the convenience of increasing the length of the pipe, which leads to an increase in the costs.

In the sixth step, the comparison has been carried out between Combo 11, Combo 6, and Combo 12 with thermal conductivities equal to 1–3 W/mK, respectively. The aim is the investigation of different thermal conductivities affecting the TOP, considering a system characterized by a number of two pipes for room with a single pipe flow rate of 225 m^3/h and 50 m length.

3. Results and Discussion

3.1. The First Step: Different Ground Thermal Conductivity Evaluation (No Geothermal System)

This step investigates an extreme case, with no geothermal system and no natural ventilation. Three values of ground thermal conductivities (1–3 W/mK) have been considered to evaluate the building behaviour, in particular the slab on ground floor (Combo 1, Combo 2, and Combo 3).

The resulting TOP trends are shown in Figure 4. The graphs point out the TOP during the summer week, from 27 July to 2 August, and for the winter week, from 14–20 January.
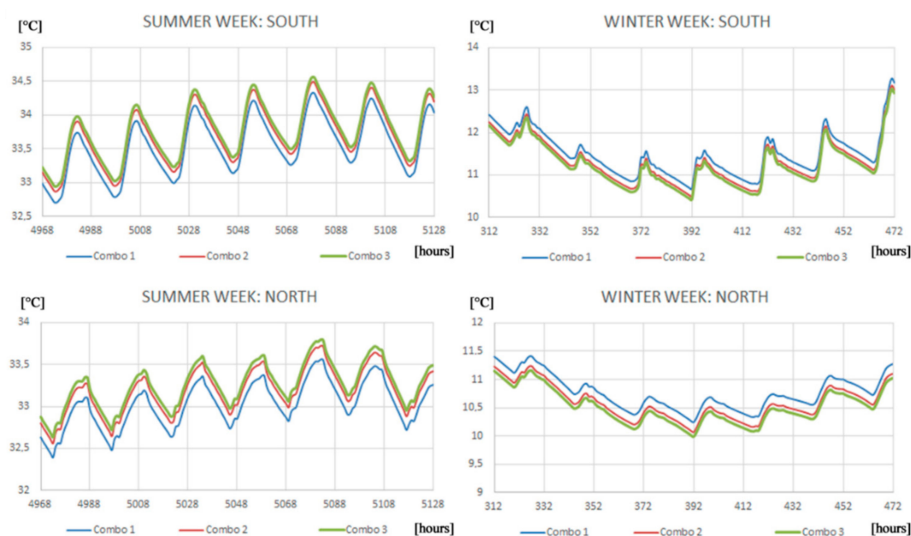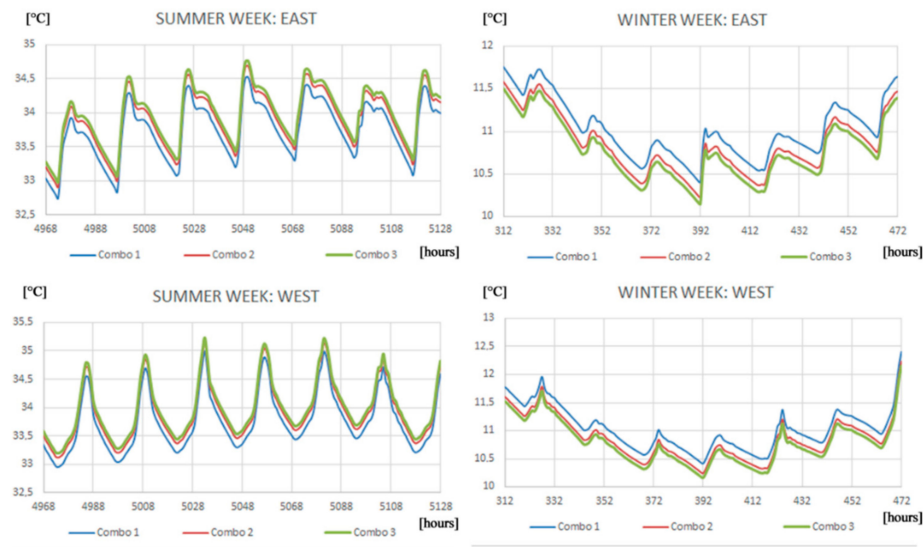

Figure 4. *Cont.*

Figure 4. TOP trend for Combo 1, 2, and 3 (27 July–2 August; 14–20 January).

Results highlight that a favourable TOP trend is obtained with a lower ground conductivity. A lower thermal conductivity of the superficial ground layer permits to have a lower temperature in the first meters of depth in summer. The best combination is obtained with a lower thermal conductivity in the superficial layer and a higher value in the deep layers. A lower TOP trend in summer is reached with Combo 1, which is characterized by a thermal ground conductivity equal to 1 W/mK. In winter, a higher TOP trend is reached with Combo 1, again. Table 8 shows the annual lowest and highest TOP peaks for each combination.

This table has been split into two different parts, the winter (blue colour) and summer (red colour) TOP peaks. The peaks are the absolute values reached by the selected combination for each orientation, the values correspond to different days of the year. It is possible to note that the northwest orientation is the coldest, while the west the hottest one. Combo 1, with ground thermal conductivity equal to 1 W/mK, presents the lowest peaks in summer and the highest peaks in winter for each orientation, resulting the most performant compared with Combo 2 (2W/mK) and Combo 3 (3 W/mK).

Table 8. First step: TOP yearly peaks (in bold lowest values in winter and highest values in summer).

				Winter TOP Peaks (°C)					
Combo	**TOP_S**	**TOP_SE**	**TOP_W**	**TOP_E**	**TOP_N**	**TOP_SW**	**TOP_CENTRAL**	**TOP_NW**	**TOP_NE**
Combo 1	10.67 17 January (8:00)	10.33 17 January (8:00)	10.42 17 January (8:00)	10.40 17 January (8:00)	10.24 16 February (7:00)	10.34 17 January (8:00)	10.80 18 January (8:00)	9.95 16 February (7:00)	9.98 17 January (8:00)
Combo 2	10.50 17 January (8:00)	10.17 17 January (8:00)	10.24 17 January (8:00)	10.23 17 January (8:00)	10.07 17 January (8:00)	10.18 17 January (8:00)	10.61 18 January (8:00)	9.81 17 January (8:00)	9.82 17 January (8:00)
Combo 3	10.42 17 January (8:00)	10.10 17 January (8:00)	10.17 17 January (8:00)	10.15 17 January (8:00)	9.99 17 January (8:00)	10.11 17 January (8:00)	10.52 18 January (8:00)	9.73 17 January (8:00)	9.75 17 January (8:00)
				Summer TOP Peaks (°C)					
Combo	**TOP_S**	**TOP_SE**	**TOP_W**	**TOP_E**	**TOP_N**	**TOP_SW**	**TOP_CENTRAL**	**TOP_NW**	**TOP_NE**
Combo 1	34.56 21 August (14:00)	34.35 21 August (14:00))	35.00 29 July (17:00)	34.53 30 July (10:00)	33.56 31 July (18:00)	34.52 31 August (16:00)	34.16 31 July (20:00)	33.70 31 July (17:00)	33.48 30 July (10:00)
Combo 2	34.69 21 August (14:00)	34.47 21 August (14:00)	35.16 29 July (17:00)	34.69 30 July (10:00)	33.72 31 July (18:00)	34.61 31 August (16:00)	34.34 31 July (20:00)	33.85 31 July (17:00)	33.63 30 July (10:00)
Combo 3	34.75 21 August (14:00)	34.52 21 August (14:00)	35.23 29 July (17:00)	34.76 30 July (10:00)	33.80 31 July (18:00)	34.66 31 August (16:00)	34.42 31 July (20:00)	33.92 31 July (17:00)	33.70 30 July (10:00)

3.2. The Second Step: Natural Ventilation with Different Ground Thermal Conductivities
(No Geothermal System)

The analysis derived the TOP in each room considering a natural ventilation equal to 160 m³/h and the influence of the building, in particular the slab on ground floor, by varying the ground thermal conductivity. The comparison has been done between Combo 1v, Combo 2v, and Combo 3v, as shown in Figure 5.
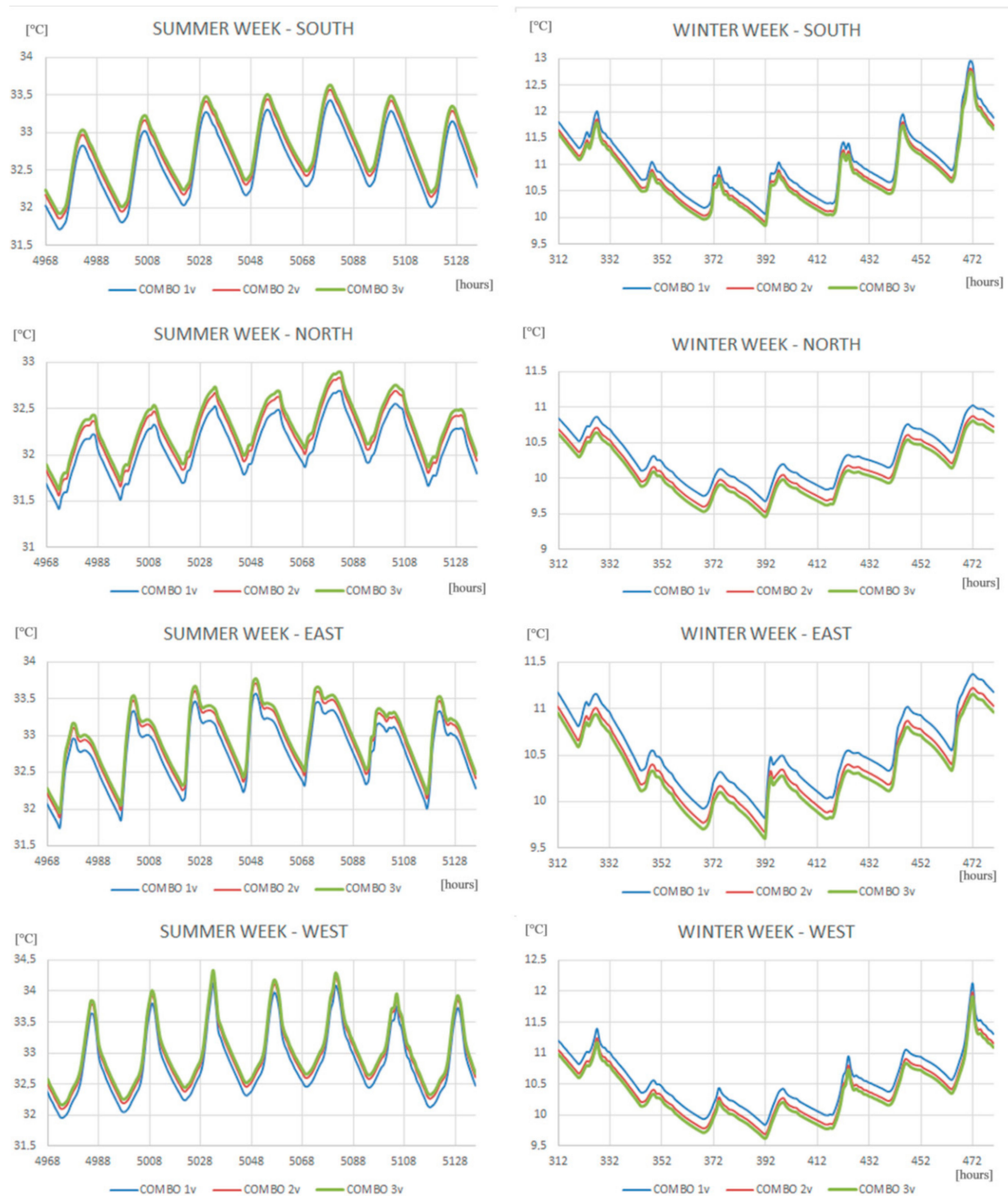
Figure 5. TOP trend for Combo 1v, 2v, and 3v (27 July–2 August; 14 January–20 January).

The comparison between Step 1 and Step 2 highlighted how the natural ventilation permits to lower the temperature by almost one degree, both in summer and winter. Again, Combo 1 (1 W/mK) shows the best behaviour in both summer and winter, while Combo 2 (2 W/mK) and Combo 3 (3 W/mK) show a very similar trend. The peaks of the TOP during the entire year are shown in Table 9.

Table 9. Second step: TOP yearly peaks.

Winter TOP Peaks (°C)									
Combo	**TOP_S**	**TOP_SE**	**TOP_W**	**TOP_E**	**TOP_N**	**TOP_SW**	**TOP_CENTRAL**	**TOP_NW**	**TOP_NE**
Combo 1v	10.07 17 January (8:00)	9.79 17 January (8:00)	9.84 17 January (8:00)	9.83 17 January (8:00)	9.68 17 January (8:00)	9.79 17 January (8:00)	10.17 17 January (8:00)	9.45 17 January (8:00)	9.44 17 January (8:00)
Combo 2v	9.92 17 January (8:00)	9.65 17 January (8:00)	9.69 17 January (8:00)	9.67 17 January (8:00)	9.53 17 January (8:00)	9.66 17 January (8:00)	10.01 17 January (8:00)	9.31 17 January (8:00)	9.30 17 January (8:00)
Combo 3v	9.86 17 January (8:00)	9.58 17 January (8:00)	9.62 17 January (8:00)	9.61 17 January (8:00)	9.46 17 January (8:00)	9.59 17 January (8:00)	9.93 17 January (8:00)	9.25 17 January (8:00)	9.24 17 January (8:00)
Summer TOP Peaks (°C)									
Combo	**TOP_S**	**TOP_SE**	**TOP_W**	**TOP_E**	**TOP_N**	**TOP_SW**	**TOP_CENTRAL**	**TOP_NW**	**TOP_NE**
Combo 1v	33.65 21 August (14:00)	33.51 21 August (14:00)	34.13 29 July (17:00)	33.57 30 July (10:00)	32.69 31 July (18:00)	33.68 31 August (16:00)	33.18 31 July (20:00)	32.89 31 July (17:00)	32.66 30 July (10:00)
Combo 2v	33.76 21 August (14:00)	33.61 21 August (14:00)	34.27 29 July (17:00)	33.71 30 July (10:00)	32.83 31 July (18:00)	33.77 31 August (16:00)	33.33 31 July (20:00)	33.02 31 July (17:00)	32.79 30 July (10:00)
Combo 3v	33.80 21 August (14:00)	33.66 21 August (14:00)	34.34 29 July (17:00)	33.77 30 July (10:00)	32.90 31 July (18:00)	33.80 31 August (16:00)	33.40 31 July (20:00)	33.08 31 July (17:00)	32.85 30 July (10:00)

In winter, the Northeast orientation reaches the lowest TOP peaks, differently from the previous case, where the lowest peaks were in the Northwest room. In summer, the highest peaks are in the West room, in accordance with the unventilated case. Again, Combo with ground thermal conductivity equal to 1 W/mK results the best solution both in winter and in summer.

3.3. The Third Step: Analysis of Different Single Pipe Flow Rates

This step investigates different pipe flow rates to evaluate the TOP in each room in combinations having the same number of pipes, length and ground thermal conductivity. Combo 2, Combo 2v, Combo 4, Combo 5, and Combo 6 have been evaluated. The aim is the analyses of the TOP variations for the following air flow rates through the pipes: 150 m^3/h (Combo 4), 187.5 m^3/h (Combo 5), 225 m^3/h (Combo 6). Combo 2 and Combo 2v are considered to enlighten the improvements obtained by the use of HAGHE compared with the extreme limit and real case, presented previously. The TOP graphs are shown in Figure 6.

Figure 6. TOP trend for Combos 2, 2v, 4, 5, and 6, and the external air temperature (27 July–2 August; 14 January–20 January).

By the analysis of Combo 2v, it possible to note that the natural ventilation makes the system more performing also in winter. The TOP of Combo 2 is often higher the TOP with HAGHE.

In summer, results highlight that Combo 4, with the lowest pipe flow rate, shows the highest TOP values inside the building while Combo 6, with the lowest pipe flow rate, shows the lowest one.

In winter, looking at the trend of Combo 2, the use of HAGHE seems to be not performing sufficiently to assure a proper indoor temperature, because the target is to get TOP as high as possible. However, this represents a limit case, completely sealed, for this reason the TOP results higher.

A flow rate of 225 m^3/h is able to further decrease the TOP in summer compared with the flow rates of 187.5 m^3/h and 150 m^3/h. A flow rate of 225 m^3/h decreases the temperature also in winter. A flow rate of 150 m^3/h causes a lower decrease of the TOP in winter. Results show that the geothermal system is not as convenient in winter as in summer, but it is possible to install a bypass to use the HAGHE system only when the ground temperature is lower than the external one.

A further analysis has been done on the temperature along the pipe in the coldest and warmest hours, as shown in Figures 7 and 8.
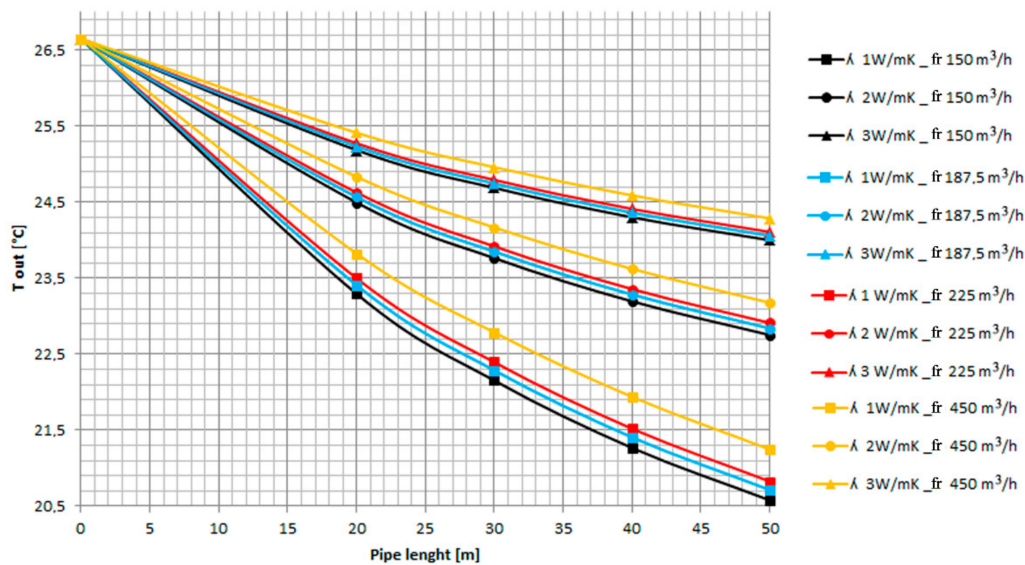

Figure 7. Air temperature along the pipe in the warmest hour (20 July, at hour 15).
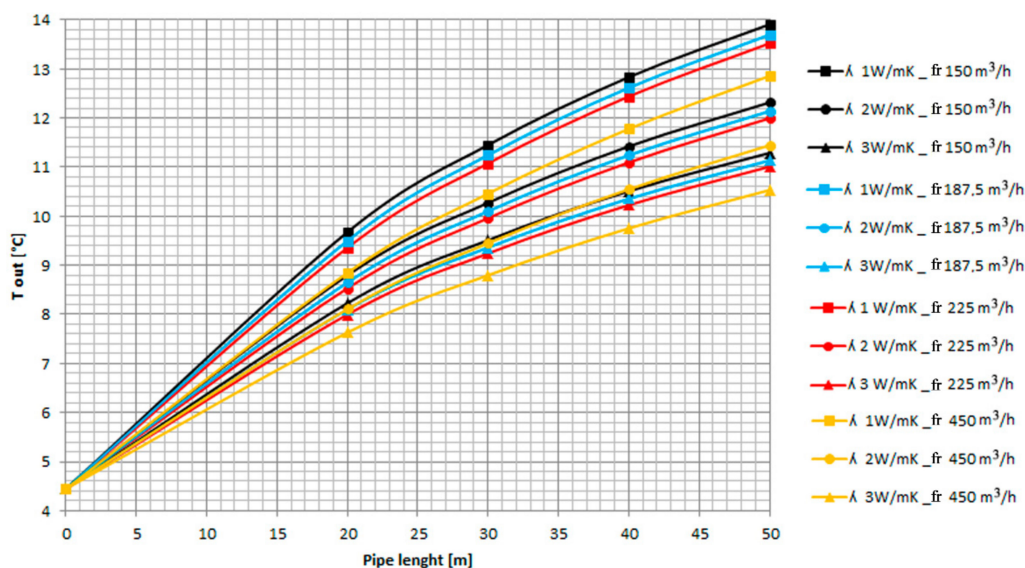

Figure 8. Air temperature along the pipe in the coldest hour (24 December, at hour 9).

Figure 7 shows the outlet temperature from the pipe, for different pipe flow rates and ground thermal conductivities during the warmest hour of summer. The curves are influenced by the thermal conductivity of the ground, as previously explained. Furthermore, from the analysis of the single pipe flow rate, is evident that low values of pipe flow rate lead a reduction of the outlet temperature.

As shown in Figure 8, the trends of the temperature along the pipe, in coldest hours, confirms the best performances of low values of ground thermal conductivity and low pipe flow rate. The major increment of the temperature is evident in the first part of the pipe.

Figures 9 and 10 show the ground-air heat flux of a single pipe, for the more critical summer and winter weeks, respectively. The results showed, for brevity, have been carried out for with the ground thermal conductivity equal to 2 W/mK, air flow rates of 150 m^3/h and 450 m^3/h and pipes with lengths of 30 m and 50 m.
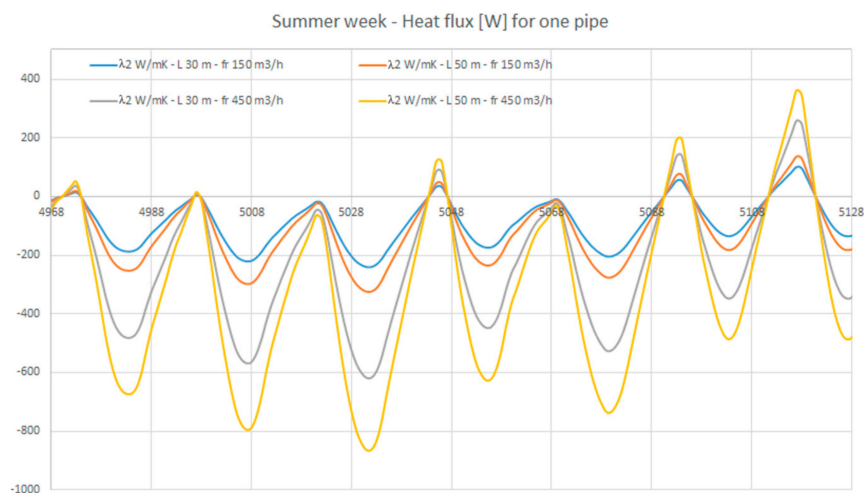
Figure 9. Heat flux [W] for one pipe during the summer week (27 July–2 August).
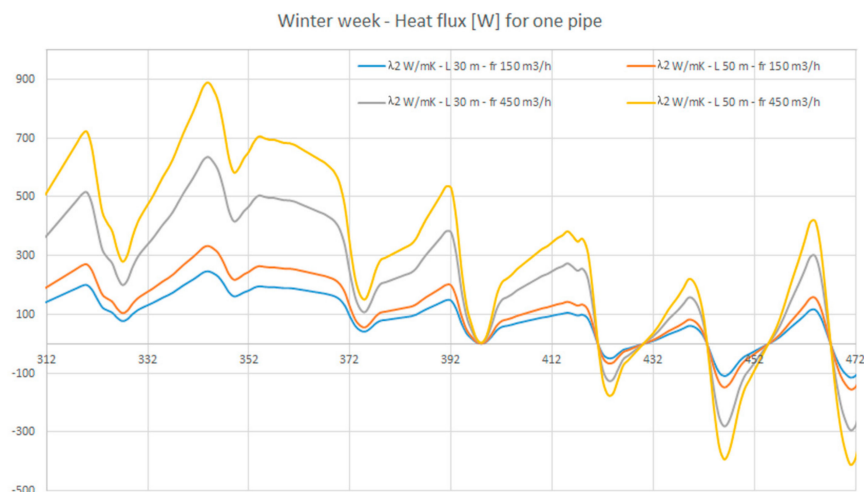
Figure 10. Heat flux [W] for one pipe during the winter week (14–20 January).

In summer, flowing into the pipe, the air suffers a cooling treatment at constant pressure. Such a condition produces an increase in relative humidity and it is necessary to provide a dehumidification post-treatment. Table 10 show the relative humidity inside the pipe, in the hottest period, for Combo 4 and Combo 6, in order to study the performance of a pipe characterized by an air flow rate equal to 150 m^3/h and the same pipe with 225 m^3/h of air flow rate. The columns UR$_{out}$ show high values. The value 1.00 represents the case in which there is condensation inside the pipe.

Table 10. Relative humidity inside the pipe.

Yearly Hours	Daily Hours	T ext (°C)	UR ext	T out Combo 4	UR out Combo 4	T out Combo 6	UR out Combo 6	Yearly Hours	Daily Hours	T ext (°C)	UR ext	T out Combo 4	UR out Combo 4	T out Combo 6	UR out Combo 6
4976	8	24.15	0.90	22.69	0.98	22.75	0.98	5072	8	25.25	0.80	23.37	0.89	23.45	0.88
4977	9	25.1	0.80	22.97	0.89	23.05	0.89	5073	9	26.35	0.60	23.68	0.67	23.79	0.67
4978	10	26.15	0.80	23.27	0.96	23.39	0.89	5074	10	27.35	0.60	23.97	0.73	24.11	0.60
4979	11	27.2	0.90	23.57	1.00	23.72	1.00	5075	11	28.2	0.60	24.22	0.76	24.38	0.75
498	12	28.05	0.80	23.82	1.00	23.99	1.00	5076	12	28.95	0.60	24.43	0.78	24.62	0.77
4981	13	28.65	0.70	23.99	0.92	24.18	0.89	5077	13	29.55	0.50	24.61	0.66	24.81	0.66
4982	14	29	0.70	24.09	0.92	24.30	0.92	5078	14	30	0.50	24.74	0.66	24.96	0.66
4983	15	29.15	0.60	24.14	0.79	24.35	0.78	5079	15	30.3	0.60	24.83	0.79	25.05	0.79
4984	16	29.15	0.70	24.15	0.92	24.35	0.92	508	16	30.3	0.60	24.83	0.79	25.06	0.79
4985	17	28.95	0.80	24.09	1.00	24.29	1.00	5081	17	30.05	0.70	24.77	0.92	24.98	0.90
4986	18	28.45	0.80	23.96	1.00	24.14	1.00	5082	18	29.6	0.70	24.64	0.92	24.85	0.92
4987	19	27.65	1.00	23.73	1.00	23.89	1.00	5083	19	28.9	0.80	24.45	1.00	24.63	1.00
4988	20	26.9	1.00	23.52	1.00	23.66	1.00	5084	20	28.05	0.90	24.21	1.00	24.37	1.00
5	8	24.65	0.70	22.93	0.78	23.00	0.77	5096	8	22.6	0.60	22.70	0.60	22.70	0.60
5001	9	25.95	0.60	23.30	0.67	23.41	0.67	5097	9	23.6	0.50	22.99	0.50	23.02	0.50
5002	10	27.15	0.60	23.64	0.74	23.79	0.73	5098	10	24.65	0.50	23.29	0.50	23.35	0.50
5003	11	28.2	0.60	23.95	0.77	24.12	0.76	5099	11	25.5	0.50	23.54	0.56	23.62	0.50
5004	12	29.15	0.60	24.22	0.79	24.42	0.79	51	12	26.3	0.50	23.77	0.56	23.87	0.56
5005	13	29.9	0.50	24.44	0.66	24.66	0.66	5101	13	27	0.50	23.97	0.56	24.10	0.56
5006	14	30.35	0.50	24.57	0.66	24.81	0.66	5102	14	27.5	0.60	24.12	0.73	24.26	0.73
5007	15	30.55	0.60	24.63	0.85	24.87	0.79	5103	15	27.8	0.60	24.21	0.74	24.35	0.73
5008	16	30.5	0.70	24.62	0.99	24.86	0.97	5104	16	27.8	0.60	24.21	0.74	24.36	0.73
5009	17	30.1	0.60	24.51	0.79	24.74	0.79	5105	17	27.5	0.60	24.13	0.67	24.27	0.67
501	18	29.4	0.70	24.32	0.92	24.53	0.92	5106	18	26.95	0.80	23.98	0.95	24.10	0.95
5011	19	28.5	0.80	24.07	1.00	24.25	1.00	5107	19	26.2	0.90	23.77	1.00	23.87	1.00
5012	20	27.7	0.80	23.84	1.00	24.00	1.00	5108	20	25.4	1.00	23.55	1.00	23.62	1.00
5024	8	25.4	0.70	23.23	0.78	23.32	0.78	512	8	21.75	0.40	22.55	0.40	22.52	0.40
5025	9	26.75	0.70	23.62	0.84	23.75	0.78	5121	9	23.1	0.40	22.93	0.40	22.94	0.40
5026	10	28	0.70	23.98	0.89	24.14	0.88	5122	10	24.35	0.50	23.29	0.50	23.34	0.50
5027	11	29.1	0.80	24.29	1.00	24.49	1.00	5123	11	25.5	0.50	23.62	0.51	23.70	0.56
5028	12	30	0.80	24.55	1.00	24.78	1.00	5124	12	26.5	0.50	23.91	0.56	24.02	0.56
5029	13	30.7	0.80	24.76	1.00	25	1.00	5125	13	27.25	0.40	24.13	0.44	24.26	0.44
503	14	31.15	0.70	24.89	1.00	25.14	0.99	5126	14	27.75	0.40	24.27	0.44	24.42	0.44
5031	15	31.4	0.60	24.96	0.87	25.23	0.84	5127	15	27.95	0.40	24.34	0.44	24.48	0.44
5032	16	31.4	0.70	24.97	1.00	25.23	0.98	5128	16	27.9	0.40	24.33	0.44	24.47	0.44
5033	17	31.1	0.70	24.89	1.00	25.14	0.99	5129	17	27.5	0.30	24.22	0.33	24.35	0.33
5034	18	30.45	0.80	24.71	1.00	24.94	1.00	513	18	26.75	0.40	24.01	0.44	24.12	0.44

Table 10. *Cont.*

Yearly Hours	Daily Hours	T ext (°C)	UR ext	T out Combo 4	UR out Combo 4	T out Combo 6	UR out Combo 6	Yearly Hours	Daily Hours	T ext (°C)	UR ext	T out Combo 4	UR out Combo 4	T out Combo 6	UR out Combo 6
5035	19	29.5	0.90	24.44	1.00	24.65	1.00	5131	19	25.8	0.50	23.74	0.56	23.83	0.50
5036	20	28.6	0.90	24.19	1.00	24.37	1.00	5132	20	24.9	0.60	23.49	0.60	23.55	0.60
5048	8	23.5	0.70	22.78	0.70	22.81	0.70	-	-	-	-	-	-	-	-
5049	9	24.85	0.60	23.17	0.66	23.24	0.61	-	-	-	-	-	-	-	-
505	10	26	0.60	23.50	0.67	23.60	0.67	-	-	-	-	-	-	-	-
5051	11	26.95	0.60	23.77	0.72	23.90	0.67	-	-	-	-	-	-	-	-
5052	12	27.8	0.70	24.02	0.88	24.17	0.87	-	-	-	-	-	-	-	-
5053	13	28.45	0.60	24.21	0.77	24.38	0.76	-	-	-	-	-	-	-	-
5054	14	28.85	0.80	24.33	1.00	24.51	1.00	-	-	-	-	-	-	-	-
5055	15	29.05	0.80	24.39	1.00	24.58	1.00	-	-	-	-	-	-	-	-
5056	16	29	0.70	24.38	0.92	24.57	0.91	-	-	-	-	-	-	-	-
5057	17	28.65	0.60	24.28	0.78	24.46	0.77	-	-	-	-	-	-	-	-
5058	18	28	0.70	24.10	0.88	24.26	0.87	-	-	-	-	-	-	-	-
5059	19	27.1	0.80	23.85	0.97	23.98	0.96	-	-	-	-	-	-	-	-
506	20	26.35	0.90	23.64	1.00	23.75	1.00	-	-	-	-	-	-	-	-

3.4. The Fourth Step: Evaluation of the Number of Pipes

The aim of this step is the analysis of the number of pipes for each room, considering the same total pipe flow rate. This step investigates Combo 6 and Combo 7. Combo 6 consists of two pipes of 50 m length in each room with a single pipe flow rate equal to 225 m^3/h for a total pipe flow rate of 4050 m^3/h. Combo 7 has four pipes of 25 m length for each room with a single pipe flow rate equal to 112.5 m^3/h for a total pipe flow rate of 4050 m^3/h. Results are presented in Figure 11. As shown, the best solution in terms of TOP, both in summer and winter, is obtained with Combo 6.
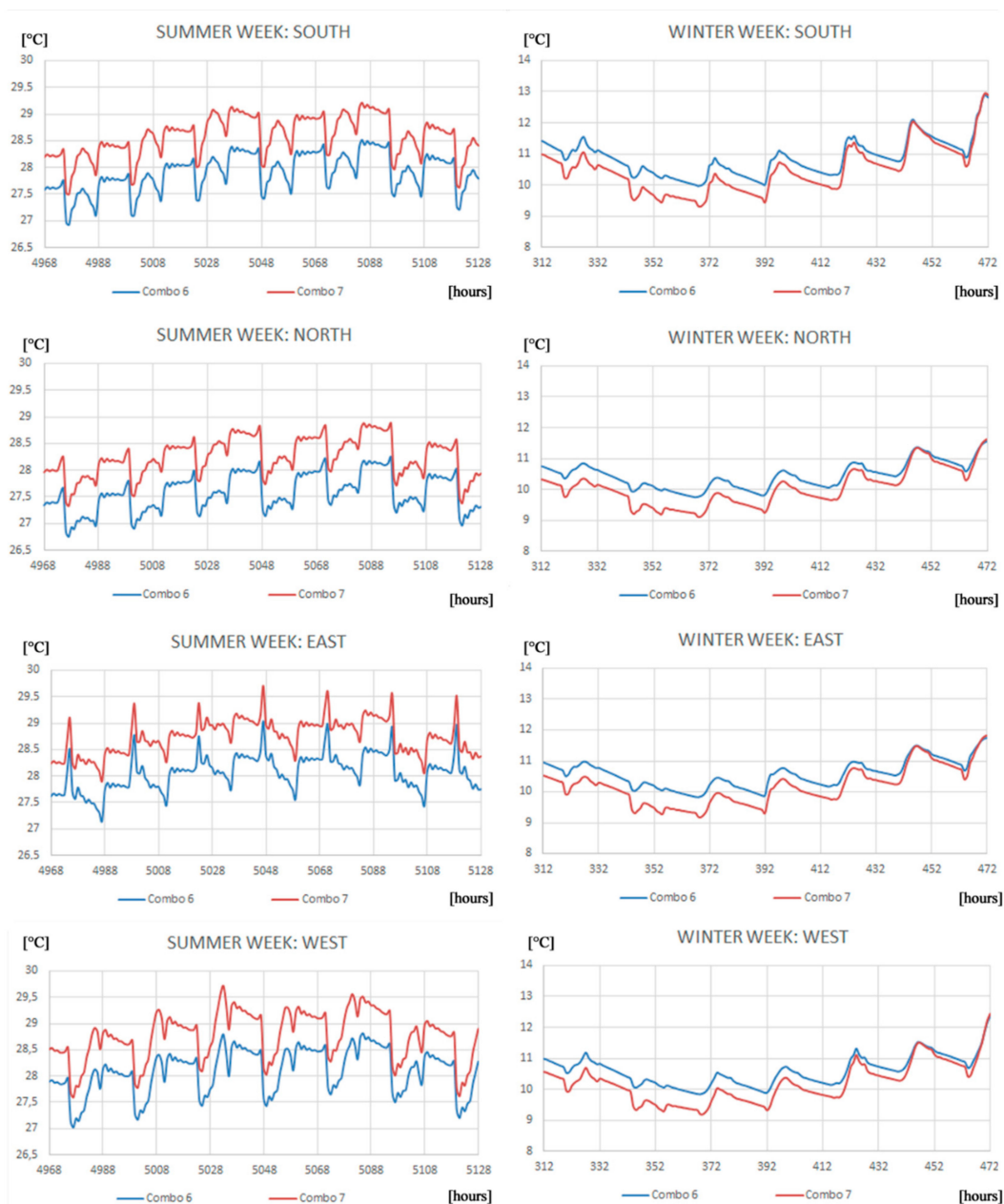
Figure 11. TOP trend for Combos 6 and 7 (27 July–2 August; 14–20 January).

The TOP peaks reached by the analysis of Combo 6 and Combo 7 have been studied in summer and winter conditions and reported in Table 11.

Table 11. Fourth step: TOP yearly peaks (in bold lowest values in winter and highest values in summer).

Winter TOP peaks (°C)								
Combo	**TOP_S**	**TOP_SE**	**TOP_W**	**TOP_E**	**TOP_N**	**TOP_SW**	**TOP_CENTRAL**	**TOP_NW**	**TOP_NE**
Combo 6	9.10 16 February (8:00)	9.10 16 February (8:00)	8.72 16 February (8:00)	9.05 16 February (8:00)	8.56 16 February 16 (8:00)	8.95 16 February (8:00)	8.91 16 February (8:00)	8.44 16 February (8:00)	8.43 15 February (8:00)
Combo 7	9.05 16 February (8:00)	9.05 16 February (8:00)	8.67 16 February (8:00)	9.00 16 February (8:00)	8.51 16 February (8:00)	8.90 16 February (8:00)	8.86 16 February (8:00)	8.39 15 February (8:00)	8.20 14 February (8:00)

Summer TOP peaks (°C)								
Combo	**TOP_S**	**TOP_SE**	**TOP_W**	**TOP_E**	**TOP_N**	**TOP_SW**	**TOP_CENTRAL**	**TOP_NW**	**TOP_NE**
Combo 6	29.71 31 August (14:00)	29.81 31 August (14:00)	29.97 31 August (17:00)	29.65 September 1 (7:00)	29.34 20 August (7:00)	29.93 31 August (16:00)	29.54 20 August (7:00)	29.37 20 August (7:00)	29.36 20 August (7:00)
Combo 7	30.14 31 August (14:00)	30.23 31 August (14:00)	30.54 18 August (17:00)	30.17 23 July (7:00)	29.79 20 August (7:00)	30.38 31 August (16:00)	30.04 20 August (7:00)	29.80 20 August (7:00)	29.78 20 August (7:00)

As shown, from the comparison between Combo 6 and Combo 7, the lower value of TOP reached during the entire year is equal to 8.20 °C by Combo 7 at a northeast orientation. With the same orientation, Combo 6 reaches the value of 8.42 °C, considered the lower value of Combo 6. The Northeast orientation shows the greatest difference between TOP winter peaks, resulting equal to 0.22 °C. The minor difference in temperature is in the east-oriented room equal to 0.04 °C.

In Combo 7, the warmest room is positioned to West where a TOP value of 30.54 °C is reached. This value falls to 29.97 °C in Combo 6. This orientation reports also the greatest difference in TOP summer peaks between Combo 6 and Combo 7, resulting equal to 0.58 °C, while the minor difference is at southwest orientation (0.42 °C).

Having the same total mass flow rate, the most favourable result is found with a 50 m pipe. This finding underlines the importance of the heat transfer convective coefficient due to the higher air velocity.

3.5. The Fifth Step: Study of the Length of the Pipe

The comparison has been done among Combos 6, 8, 9, and 10. The aim of this step is the comparison of combinations with different length, and equal number of pipes, pipe flow rate and thermal conductivity of the ground. The pipe length ranges from 20 m to 50 m, as shown in Figure 12.
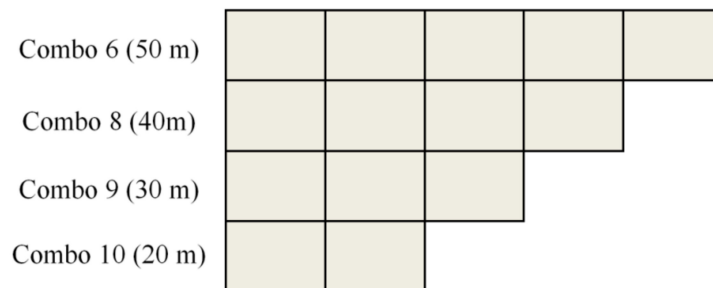
Figure 12. Pipe length of the combos compared in the fifth step.

The TOP graphs related to this step are shown in Figure 13.
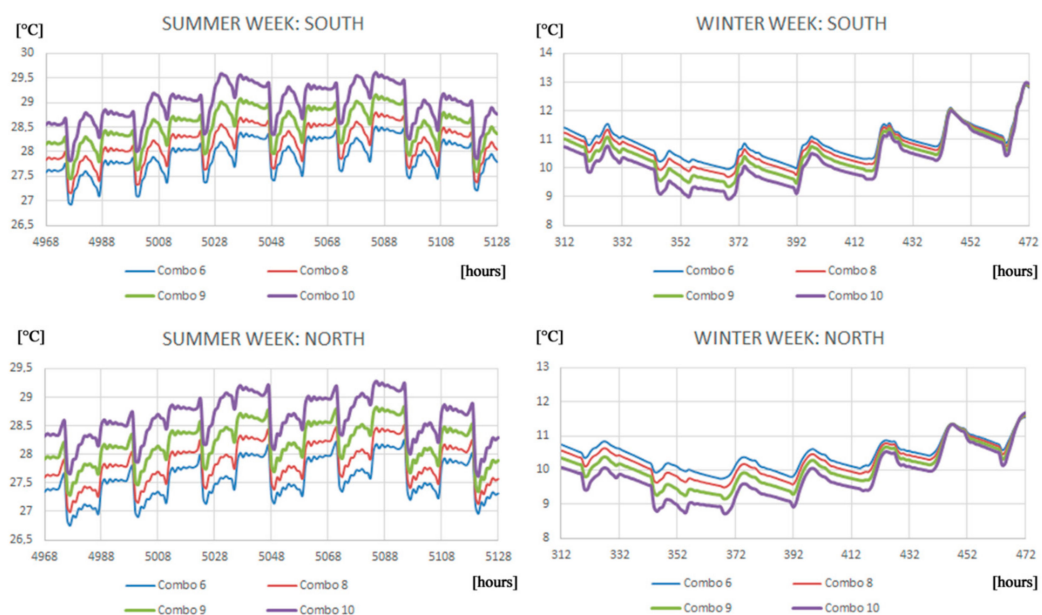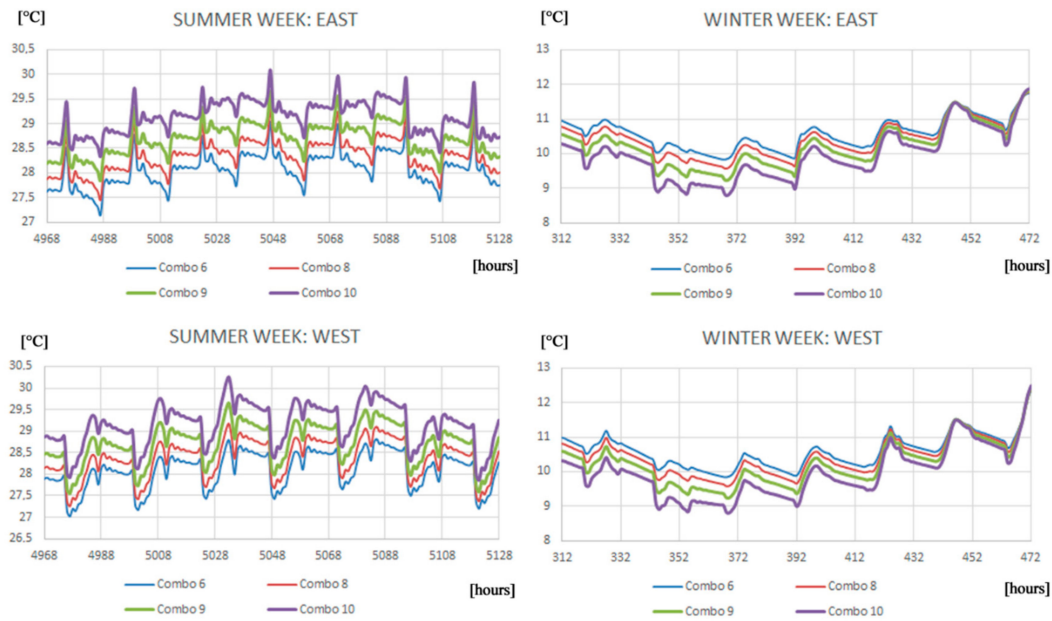

Figure 13. *Cont.*

Figure 13. TOP trend for Combos 6, 8, 9, and 10 (27 July–2 August; 14 January–20 January).

In summer, Combo 10 presents the highest TOP values inside the building while Combo 6 has the lowest. The hottest room in Combo 10 (2 pipes of 20 m) is west-oriented and has a temperature of 30.93 °C. The same temperature is 29.97 °C in Combo 6.

In winter, Combo 6 and Combo 10 show, respectively, the maximum and minimum TOP during the coldest day. A temperature of 8.05 °C is found in Combo 10. Results show that a 50 m pipe is preferable to improve the internal comfort, compared to shorter pipes that are suggested only with a ground thermal conductivity close to 3 W/mK. A plot related to the temperature at the HAGHE outlet is shown in Figure 14 in relation to Combo 10.
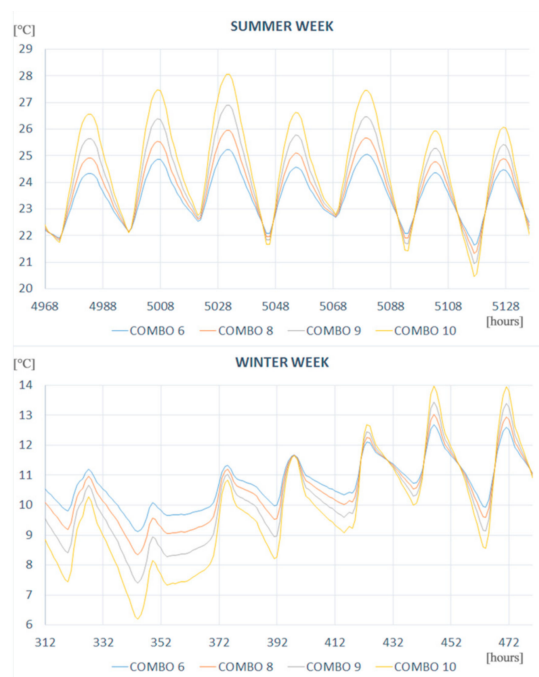
Figure 14. Trend of for Combos 6, 8, 9, and 10 (27 July–2 August; 14–20 January) for the outlet temperature Tout from the geothermal system.

The increase of the pipe length implies a decrease of the air temperature coming out from the pipe in summer and an increase in winter, but the major temperature drop takes place in the first meters through the soil. A further length increases up from 30 m to 50 m involves an additional decrease of only 0.52 °C but a length of 50 m is more expensive. Thus, a length of 30 m shows a good performance, reducing the stretch of pipe working with a small air-ground temperature difference.

3.6. The Sixth Step: Different Ground Thermal Conductivity Evaluation (Geothermal System)

The aim of this step is the evaluation of the behaviour of the HAGHE considering different ground thermal conductivities, equal to 1, 2, and 3 W/mK. Combo 6, Combo 11, and Combo 12, compared in this step, are characterized by two pipes for room with a single pipe flow rate of 225 m³/h and 50 m length. Figure 15 shows the comparison between the TOP trends at each orientation.
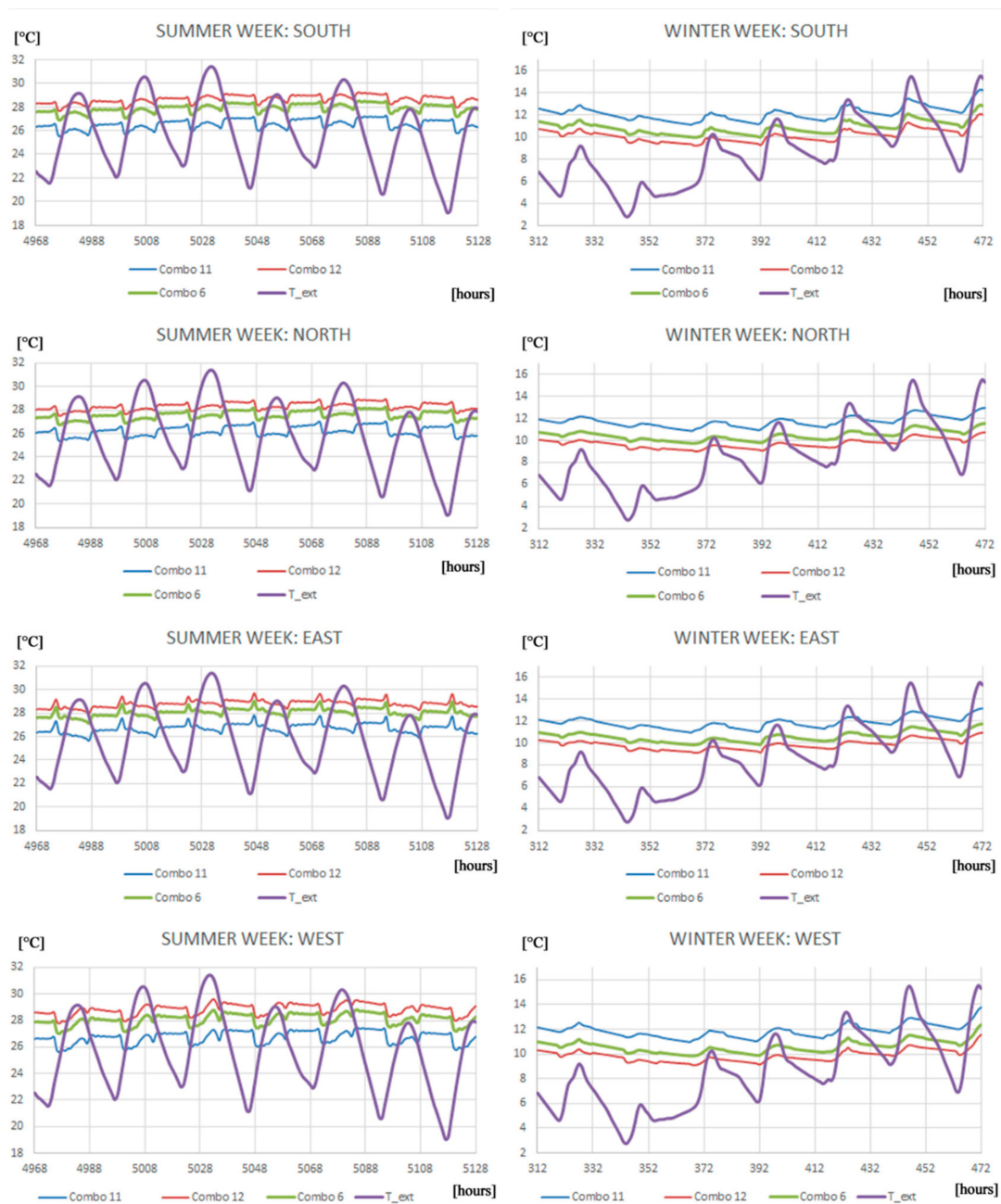

Figure 15. TOP trend for Combos 6, 11, 12, and external air temperature (27 July–2 August; 14–20 January).

The graphs show a better trend of Combo 11, with thermal conductivity equal to 1 W/mK. Combo 12, with thermal conductivity equal to 3 W/mK, is characterized by a strong exchange between the ground and the external environment, due to the lower capacity of the ground to work as an insulating layer. The strong exchange between the external environment and the ground involves higher TOP values in summer and lower in winter, compared with Combo 11.

4. Conclusions

Topic of this work is to understand the behavior of a building, located in a warm climate, without a traditional HVAC system, but provided only a ventilation system coupled with a horizontal air-ground heat exchanger. Of course, such a system cannot completely supply the thermal loads, in terms of temperature and relative humidity, but it can strongly mitigate the internal thermal conditions with really low operative costs, just the energy consumption for the ventilation.

The paper presents a methodology for the evaluation of the operative air temperature (TOP) for different ventilation system configurations. A climatization given by a horizontal air-ground heat exchanger (HAGHE) is verified testing different system options, like the pipe numbers, air flow rate, soil thermal conductivity, and pipe depth. Starting from an optimized envelope for the investigated climate analyzed in a previous study [30], results show that the internal loads can be decreased, and the air-conditioning provided only by a HAGHE suitable for the investigated climate.

Results highlight that a favorable TOP trend is obtained with a lower ground conductivity (1 W/mK). The heat flux exchanged between the floor and ground is higher because of a lower ground temperature in both summer and winter. In particular, a lower conductivity of the superficial ground layer permits to have a lower temperature in the first meters of depth in summer.

Results show that pipes with a high air mass flow rate are able to reduce the temperature peaks on the internal side of the building. A lower number of pipes are preferable given the same air flow and implant length, while a higher length is preferable given the same total air flow and pipes number.

Further studies may be developed to identify the optimal solution in terms of costs and thermal performance. Another future research development can be related to the investigation of other climates.

Author Contributions: Work plan, P.M.C.; Simulations, C.B.; Analysis of result: C.B., D.D. and P.M.C.; Writing: D.D.; Revision of the manuscript: P.M.C.

Conflicts of Interest: The authors declare no conflict of interest.

Nomenclature

TOP	Operative air temperature (°C)
HVAC	Heating, Ventilation and Air Conditioning
HAGHE	Horizontal Air-Ground Heat Exchangers
U	Steady thermal transmittance (W/m^{2}K)
Y_{mm}	Thermal admittance (W/m^{2}K)
Y_{mn}	Periodic thermal transmittance (W/m^{2}K)
c	Specific heat capacity (J/kgK)
d	Thickness of a layer (m)
fd	Decrement factor
g	Solar factor
t	Time shift: time lead (if positive), or time lag (if negative) (s or h)
Ms	Total surface mass (excluding coats) (Kg/m^2)
fr	Flow rate (m^3/h)
Subscripts	
m, n	For the thermal zones
g	Glass
f	Frame

1	Internal
2	External
22	From environment to environment

References

1. Taking Stock of the Europe 2020 Strategy for Smart, Sustainable and Inclusive Growth. Available online: https://ec.europa.eu/info/sites/info/files/europe2020stocktaking_annex_en.pdf (accessed on 12 July 2018).

2. D'Agostino, D. Assessment of the progress towards the establishment of definitions of Nearly Zero Energy Buildings (NZEBs) in European Member States. *J. Build. Eng.* **2015**, *1*, 20–32. [CrossRef]

3. D'Agostino, D.; Cuniberti, B.; Bertoldi, P. Energy consumption and efficiency technology measures in European non-residential buildings. *Energy Build.* **2017**, *153*, 72–86. [CrossRef]

4. Directive 2010/31/EU on the Energy Performance of Buildings (recast)—19 May 2010. Available online: http://www.buildup.eu/en/practices/publications/directive-201031eu-energy-performance-buildings-recast-19-may-2010 (accessed on 9 August 2018).

5. Directive 2012/27/EU of the European Parliament and of the Council of 25 October 2012 on Energy Efficiency. Available online: http://www.buildup.eu/en/practices/publications/directive-201227eu-european-parliament-and-council-25-october-2012-energy (accessed on 9 August 2018).

6. Directive 2009/28/EC of the European Parliament and of the Council of 23 April 2009 on the Promotion of the Use of Energy from Renewable Sources and Amending and Subsequently Repealing Directives 2001/77/EC and 2003/30/EC. Available online: http://www.buildup.eu/en/practices/publications/directive-200928ec-european-parliament-and-council-23-april-2009-promotion (accessed on 9 August 2018).

7. D'Agostino, D.; Zangheri, P.; Castellazzi, L. Towards Nearly Zero Energy buildings (NZEBs) in Europe: A focus on retrofit in non-residential buildings. *Energies* **2017**, *10*, 117.

8. D'Agostino, D.; Parker, D. A framework for the cost-optimal design of nearly zero energy buildings (NZEBs) in representative climates across Europe. *Energy* **2018**, *149*, 814–829. [CrossRef]

9. D'Agostino, D.; Parker, D. Data on cost-optimal Nearly Zero Energy Buildings (NZEBs) across Europe. *Data Brief.* **2018**, *17*, 1168–1174. [CrossRef] [PubMed]

10. Tian, Z.; Zhang, X.; Jin, X.; Zhou, X.; Si, B.; Shi, X. Towards adoption of building energy simulation and optimization for passive building design: A survey and a review. *Energy Build.* **2018**, *158*, 1306–1316. [CrossRef]

11. Aste, N.; Manfren, M.; Marenzi, G. Building automation and control systems and performance optimization: A framework for analysis. *Renew. Sustain. Energy Rev.* **2017**, *75*, 313–330. [CrossRef]

12. Wright, J.; Loosemore, H.; Farmani, R. Optimization of building thermal design and control by multi-criterion genetic algorithm. *Energy Build.* **2002**, *34*, 959–972. [CrossRef]

13. Bambrook, S.; Sproul, A.; Jacob, D. Design optimisation for a low energy home in Sydney. *Energy Build.* **2011**, *43*, 1702–1711. [CrossRef]

14. Vera, J.; Laukkanen, T.; Sirén, K. Multi-objective optimization of hybrid photovoltaic–thermal collectors integrated in a DHW heating system. *Energy Build.* **2014**, *74*, 78–90. [CrossRef]

15. Stavrakakis, G.; Zervas, P.; Sarimveis, H.; Markatos, N. Optimization of window-openings design for thermal comfort in naturally ventilated buildings. *Appl. Math. Model.* **2012**, *36*, 193–211. [CrossRef]

16. Rapone, G.; Saro, O. Optimisation of curtain wall facades for office buildings by means of PSO algorithm. *Energy Build.* **2012**, *45*, 189–196. [CrossRef]

17. Chantrelle, F.P.; Lahmidi, H.; Keilholz, W.; Mankibi, M.; Michel, P. Development of a multicriteria tool for optimizing the renovation of buildings. *Appl. Energy* **2011**, *88*, 1386–1394. [CrossRef]

18. Huang, S.; Hu, R. Optimum design for indoor humidity by coupling Genetic Algorithm with transient simulation based on Contribution Ratio of Indoor Humidity and Climate analysis. *Energy Build.* **2012**, *47*, 208–216. [CrossRef]

19. Chen, H.; Ooka, R.; Kato, S. Study on optimum design method for pleasant outdoor thermal environment using genetic algorithms (GA) and coupled simulation of convection, radiation and conduction. *Build. Environ.* **2008**, *43*, 18–30. [CrossRef]

20. Eisenhower, B.; O'Neill, Z.; Narayanan, S.; Fonoberov, V.A.; Mezi, I. A methodology for meta model based optimization in building energy models. *Energy Build.* **2012**, *47*, 292–301. [CrossRef]

21. Valdiserri, P.; Biserni, C.; Garai, M. Energy performance of a ventilation system for an apartment according to the Italian regulation. *Int. J. Energy Environ. Eng.* **2016**, *7*, 353–359. [CrossRef]

22. Lucchi, M.; Lorenzini, M.; Valdiserri, P. Energy performance of a ventilation system for a block of apartments with a ground source heat pump as generation system. *J. Phys. Conf. Ser.* **2017**, *796*, 1. [CrossRef]

23. Zhou, L.; Haghighat, F. Optimization of ventilation system design and operation in office environment. Part I: Methodology. *Build. Environ.* **2009**, *44*, 651–656. [CrossRef]

24. Wu, R.; Mavromatidis, G.; Orehounig, K.; Carmeliet, J. Multiobjective optimisation of energy systems and building envelope retrofit in a residential community. *Appl. Energy* **2017**, *190*, 634–649. [CrossRef]

25. Kurnitski, J.; Saari, A.; Kalamees, T.; Vuolle, M.; Niemelä, J.; Tark, T. Cost optimal and nearly zero energy performance requirements for buildings in Estonia. *Est. J. Eng.* **2013**, *19*, 183–202. [CrossRef]

26. Baglivo, C.; Congedo, P.M.; D'Agostino, D.; Zacà, I. Cost-optimal analysis and technical comparison between standard and high efficient mono-residential buildings in a warm climate. *Energy* **2015**, *83*, 560–575. [CrossRef]

27. Zacà, I.; D'Agostino, D.; Congedo, P.M.; Baglivo, C. Assessment of cost-optimality and technical solutions in high performance multi-residential buildings in the Mediterranean area. *Energy Build.* **2015**, *102*, 250–265. [CrossRef]

28. Congedo, P.M.; Baglivo, C.; D'Agostino, D.; Tornese, G.; Zacà, I. Efficient solutions and cost-optimal analysis for existing school buildings. *Energies* **2016**, *9*, 851. [CrossRef]

29. Congedo, P.M.; Baglivo, C.; D'Agostino, D.; Zacà, I. Cost-optimal design for nearly zero energy office buildings located in warm climates. *Energy* **2015**, *91*, 967–982. [CrossRef]

30. Glavič, P.; Lukman, R. Review of sustainability terms and their definitions. *J. Clean. Prod.* **2007**, *15*, 1875–1885. [CrossRef]

31. Zhou, C.; Yin, G.; Hu, X. Multi-objective optimization of material selection for sustainable products: Artificial neural networks and genetic algorithm approach. *Mater. Des.* **2009**, *30*, 1209–1215. [CrossRef]

32. Mora, E.P. Life cycle, sustainability and the transcendent quality of building materials. *Build. Environ.* **2007**, *42*, 1329–1334. [CrossRef]

33. Dammann, S.; Elle, M. Environmental indicators: establishing a common language for green building. *Build. Res. Inform.* **2006**, *34*, 387–404. [CrossRef]

34. Barreca, F. Use of giant reed Arundo Donax L. in rural constructions. *Agric. Eng. Int. CIGR J.* **2012**, *14*, 46–52.

35. Congedo, P.M.; Baglivo, C.; Zacà, I.; D'Agostino, D.; Quarta, F.; Cannoletta, A.; Marti, A.; Ostuni, V. Energy retrofit and environmental sustainability improvement of a historical farmhouse in Southern Italy. *Energy Procedia* **2017**, *133*, 367–381. [CrossRef]

36. Balivo, C.; Congedo, P.M.; Cataldo, M.D.; Coluccia, L.D.; D'Agostino, D. Envelope Design optimization by thermal modelling of a building in a warm climate. *Energies* **2017**, *10*, 1808. [CrossRef]

37. Argiriou, A. Ground cooling. In *Passive Cooling of Buildings*; Santamouris, M., Asimakopoulos, D., Eds.; Earthscan: New York, NY, USA, 2013; pp. 360–403.

38. Ascione, F.; Bellia, L.; Minichiello, F. Earth-to-air heat exchangers for Italian climates. *Renew. Energy* **2011**, *36*, 2177–2188. [CrossRef]

39. Pfafferott, J. Evaluation of earth-to-air heat exchangers with a standardised method to calculate energy efficiency. *Energy Build.* **2003**, *35*, 971–983. [CrossRef]

40. Lee, K.H.; Strand, R.K. The cooling and heating potential of an earth tube system in buildings. *Energy Build.* **2008**, *40*, 486–494. [CrossRef]

41. Genchi, Y.; Kikegawa, Y.; Inaba, A. CO_2 payback-time assessment of a regional-scale heating and cooling system using a ground source heat-pump in a high energy-consumption area in Tokyo. *Appl. Energy* **2002**, *71*, 147–160. [CrossRef]

42. Dickinson, J.; Jackson, T.; Matthews, M.; Cripps, A. The economic and environmental optimisation of integrating ground source energy systems into buildings. *Energy* **2009**, *34*, 2215–2222. [CrossRef]

43. Esen, H.; Inalli, M.; Esen, M. A techno-economic comparison of ground-coupled and air-coupled heat pump system for space cooling. *Build. Environ.* **2007**, *42*, 1955–1965. [CrossRef]

44. Keil, C.; Plura, S.; Radspieler, M.; Schweigler, C. Application of customized absorption heat pumps for utilization of low-grade heat sources. *Appl. Therm. Eng.* **2008**, *28*, 2070–2076. [CrossRef]

45. Desideri, U.; Sorbi, N.; Arcioni, L.; Leonardi, D. Feasibility study and numerical simulation of a ground source heat pump plant, applied to a residential building. *Appl. Therm. Eng.* **2011**, *31*, 3500–3511. [CrossRef]

46. Li, H.; Yang, H. Study on performance of solar assisted air source heat pump systems for hot water production in Hong Kong. *Appl. Energy* **2010**, *87*, 2818–2825. [CrossRef]

47. Chen, C.; Sun, F.-L.; Feng, L.; Liu, M. Underground water-source loop heat-pump air-conditioning system applied in a residential building in Beijing. *Appl. Energy* **2005**, *82*, 331–344. [CrossRef]

48. Lund, J.W.; Freeston, D.H.; Boyd, T.L. Direct application of geothermal energy: 2005 worldwide review. *Geothermics* **2005**, *34*, 691–727. [CrossRef]

49. Wu, Y.; Gan, G.; Verhoef, A.; Vidale, P.L.; Gonzalez, R.G. Experimental measurement and numerical simulation of horizontal-coupled slinky ground source heat exchangers. *Appl. Therm. Eng.* **2010**, *30*, 2574–2583. [CrossRef]

50. Congedo, P.; Lorusso, C.; De Giorgi, M.; Laforgia, D. Computational fluid dynamic modeling of horizontal Air-Ground Heat Exchangers (HAGHE) for HVAC Systems. *Energies* **2014**, *7*, 8465–8482. [CrossRef]

51. Congedo, P.M.; Lorusso, C.; Giorgi, M.G.D.; Marti, R.; D'Agostino, D. Horizontal air-ground heat exchanger performance and humidity simulation by computational fluid dynamic analysis. *Energies* **2016**, *9*, 930. [CrossRef]

52. Congedo, P.M.; Colangelo, G.; Starace, G. CFD simulations of horizontal ground heat exchangers: A comparison among different configurations. *Appl. Therm. Eng.* **2012**, *33*, 24–32. [CrossRef]

53. D'Agostino, D.; Congedo, P.M. CFD modeling and moisture dynamics implications of ventilation scenarios in historical buildings. *Build. Environ.* **2014**, *79*, 181–193. [CrossRef]

54. Bradley, D.; Kummert, M. New evolutions in TRNSYS—A selection of Version 16 features. In Proceedings of the Ninth International IBPSA Conference, Montréal, QC, Canada, 15–18 August 2005; pp. 107–114.